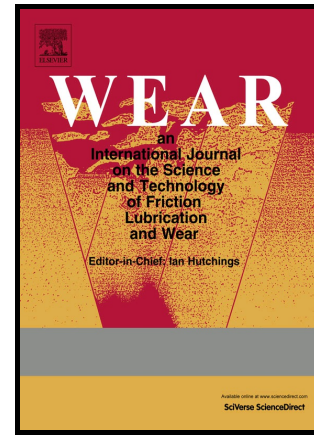# Author's Accepted Manuscript

A new methodology for measuring galling wear severity in high strength steels

Brendan Voss, Michael Pereira, Bernard Rolfe, Matthew Doolan

Cite this article as: Brendan Voss, Michael Pereira, Bernard Rolfe and Matthew Doolan, A new methodology for measuring galling wear severity in high strength steels, *Wear,* http://dx.doi.org/10.1016/j.wear.2017.09.002

A new methodology for measuring galling wear severity in high strength steels

Brendan Voss [a*], Michael Pereira [b], Bernard Rolfe [b], Matthew Doolan [a]

a) Research School of Engineering, Australian National University, Canberra, ACT 2601, Australia

b) School of Engineering, Deakin University, Locked Bag 20000, Geelong, VIC 3220, Australia

*Corresponding author email address: Brendan.Voss@anu.edu.au

Abstract

With the increased usage of Advanced High Strength Steels, galling wear has become a significant challenge for sheet metal stamping industries. Galling, in particular, can have a large economic impact due to the high costs and lost productivity associated with manual monitoring, refinishing/resurfacing damaged tooling and formed parts, and the need to apply expensive treatments or coatings to tool surfaces. This has led to a push for automated galling wear detection systems. However, developing such systems requires an accurate measurement of galling wear severity that can be easily implemented in industrial situations. Parameters used for measuring galling wear are often difficult to collect in large industrial style trials, and can be inaccurate as they are not targeted towards characterising the localised features associated with galling wear damage. In this study, a new galling wear characterisation and measurement methodology is introduced that accurately measures galling wear severity by targeting the localised features on sheet metal parts. This methodology involves calculating Discrete Wavelet Transform detail coefficients of 2D surface profiles. A case study on a series of deep drawn channel parts demonstrates the accuracy of the Discrete Wavelet Transform methodology when compared to visual assessment of galling wear severity. Based on comparison to visual assessment the presented Discrete Wavelet Transform galling wear measurement methodology outperforms other commonly used wear measures. The methodology provides a targeted, repeatable and non-subjective measure of galling wear severity. The specific outcome of this work provides an important tool for research into galling wear monitoring and detection systems in sheet metal forming, and the study of galling wear and its prevention in general.

1 Introduction

Galling wear and premature tool failure is a significant challenge in sheet metal stamping and is becoming more widespread with the increased use of Advanced- and Ultra-High Strength Steels [1]. The monitoring and assessment of galling wear on deep drawing tools and the resulting damage to formed parts is of great importance in industry, as the cost of manual quality assessment, refinishing parts, and maintenance down time is significant [2]. Measurement and characterisation of this galling wear in real deep drawing situations is a crucial component in the development and implementation of accurate real time wear monitoring systems. The techniques and parameters that have been used for quantifying and characterising galling wear are often not targeted at the localised features that contribute to and are caused by galling wear. Furthermore, these traditional techniques are not well suited for implementation in large scale industrial style stamping wear trials that are necessary for developing wear monitoring systems. This work introduces a new technique for quantifying galling wear severity using 2D profilometry measurement of the surface and analysis of this surface

information using wavelet transformation. The new technique uses wavelet transformation to isolate a wavelength bandwidth that effectively characterises the localised galling wear features in 2D surface profiles. The outcome of this study is to provide an accurate quantifiable measure of galling wear severity. This is performed via measurement of the workpiece (i.e. part) surfaces and not the tool surfaces and is therefore appropriate for application in both laboratory-based experiments and industrial style wear trials. These trials are necessary for the development of automatic galling monitoring systems needed by sheet metal stamping industries to reduce the costs associated with galling wear on stamping tools and parts.

2 Background

2.1 Galling wear measurement

Galling wear in sheet metal stamping is a localised multistage sliding wear mechanism, where material transfer occurs at initiation sites and accumulates with progressive contact. The accumulated material ploughs the opposing surface and eventually the continual accumulation of galled material can result in fracture [3–5]. Galling wear damage is characterised by macroscopic localised roughening of the surface, and the creation of protrusions above the original surface due to plastic flow of the material and material transfer [6]. Galling is the wear mechanism often seen in sheet metal stamping, particularly deep drawing, where the tooling experiences repeated sliding contact under high loads with sheet metal blanks. These contact conditions and the disparity in surface roughness and hardness between the blank material and press tooling accelerates the development of galling wear.

Galling wear in sheet metal stamping is difficult to characterise and measure because of the multistage progression of the mechanism on both contacting surfaces and the lack of targeted measures. Wear damage features that precede galling observed in sheet metal forming progress through a number of stages including: asperity smoothing and plastic deformation, abrasive damage of various scales and finally progressing to galling damage [5,7,8]. These distinct surface features can be observed on both the tooling and formed parts [9]. Characterisation is further complicated in sheet metal stamping of irregularly shaped parts, where varying contact conditions can lead to localised wear that develops at different rates. The presence of wear damage can make formed parts unfit for purpose, both functionally and aesthetically, which highlights the requirement of automatic galling wear monitoring for sheet metal stamping.

Qualitative visual assessment is often used to determine the severity of wear on tooling and parts, and remains the most ubiquitous and effective method for characterising and identifying the severity of galling wear. The effectiveness of visual assessment has led to its use in numerous wear studies, often in addition to other quantitative measures [7,8,10–21]. Due to the difficulty of assessing tooling during forming operations visual assessment of formed parts is a primary method used in industrial applications for determining if tool maintenance is required [22]. Visual assessment is widely used for determining the presence and severity of galling wear in sheet metal stamping and is used as a standard in galling test methodologies [23,24]. The ASTM G98 galling test, for example, is widely used for the assessment and ranking of galling resistance of material couples. This standard utilises subjective visual characterisation of galling and provides a qualitative assessment of galling resistance [24]. A number of issues effecting the accuracy of ASTM G98 have been discussed [25], but the subjective nature of visual assessment and the need for clear and quantitative characterisation have been highlighted [26]. It is difficult to achieve repeatable results and collect a quantifiable output using visual assessment of galling wear severity. Given this, it is important to identify a quantifiable measure of galling wear equivalent to visual assessment.

Numerical rankings of galling wear severity have been used to provide a quantitative output for visual assessment [7,20,27]. However, in these instances the assessment has been made on magnified regions

where the wear state is consistent throughout. Numerical ranking schemes are less suitable for industrial style trials as they are difficult to apply to larger contact regions with multiple localised instances of wear, and are time consuming when assessing numerous parts. Despite these issues, numerical rankings are an appropriate standard for comparing galling wear measures in small scale experimental conditions.

Mass and volume loss measurements of tooling are common methods for quantifying wear [11,14,19,28,29]. These methods are convenient for the purposes of modelling given the role of wear volume the in Archard wear equation [30], which has seen extensive usage in tool wear related studies. Mass and volume loss measurements give a direct assessment of the tooling and are simple to implement in laboratory wear test conditions. However, it is possible that the techniques can give inconsistent results as wear damage can occur without loss of mass, for example with plastic deformation [31]. Therefore, measuring mass and volume loss gives an incomplete picture of the wear process. Additionally, mass and volume measurements of wear are not suitable for progressive measurement in industrial style trials, where wear assessment is desired from part to part. It is also not possible to obtain mass measurements of large and heavy sheet metal stamping tooling that are accurate enough to identify small localised changes in wear.

3D profilometry of formed parts or tooling allows for assigning standardised texture parameter values, and provides insightful information about the state of the wear conditions. Christian and De Chiffre [16] assessed adhesive and abrasive wear using bearing curve parameters S_{pk}, S_k, and S_{vk} and worked towards the characterisation of the prominent mechanism observed. Although 3D surface analysis has the potential to provide a complete quantitative characterisation of wear, a definitive selection of parameters for galling wear quantification has not been identified.

2D profilometry can also be applied to part or tooling surfaces and several standardised 2D roughness parameters are available to give information about the wear conditions. 2D profilometry has been used for the qualitative assessment of galling tracks [8] and also for collection of quantitative data using roughness parameters such as R_a, R_z, R_y, R_p, and R_v [7,10,15,16]. One issue with utilising conventional parameters, particularly the average roughness R_a, is that they can return similar values for drastically different surface topographies [32]. 2D profilometry has also been used to measure wear track depth and estimate wear volume as a means of quantifying wear [33], however, these measures are most suitable for single wear track experiments. Fast Fourier Transform (FFT) has been applied to 2D surface profiles of galled parts in order to give a Galling Severity Index (*GSI*) [34]. This *GSI* approach assesses the 2D profiles in terms of wavelengths and takes a mean value of magnitudes within a given wavelength range, which is then normalised using a mean magnitude value for an unworn reference 2D profile. The issue with this approach is that isolating the specific wavelengths at which wear features are active is difficult as all spatial information of the profile is lost during the FFT. Additionally, taking the mean value for a range of wavelengths also has the potential for reducing or losing wear information. Despite the shortcomings of 2D roughness parameters, 2D profiles taken from parts have a distinct advantage over other methods of measuring wear. Part 2D profiles are fast to acquire, are unobtrusive in terms of press tooling, and measure the product, which is ultimately the subject of interest for industry.

Sliding abrasive wear damage produces typical cross-sectional profiles as shown by Varjoranta et. al. [35] and Yost. [33]. These typical cross-sections are characterised by shoulders of raised material pile-up on either side of the depression gouge which drops below the bulk material of the surface, seen in Figure 1. The surface features seen with galling damage exhibit similar cross-sectional features in an intensified state, larger material pile up and greater depth of gouges, shown in the 2D profiles collected by Karlsson et. al. [8]. The shallow depth of abrasive damage preceding galling damage in sheet metal stamping can often be on the same scale as bulk material asperities, which can make characterisation using 2D profilometry difficult [9]. Calculating an aggregate profile by taking the mean of multiple adjacent 2D profiles can assist with minimising the asperity noise ratio when attempting to isolate these

galling related features. It is evident that all of the galling features mentioned above share the characteristic of sudden changes in height above and below the level of the bulk material. This characteristic can be captured well by aggregate 2D surface profiles perpendicular to the sliding direction and may be utilised for possible galling wear identification and quantification.

Siefert and Babu [26] numerically described galling damage and a number of other damage stages for ASTM G98 tests in terms of R_y values for profiles collected perpendicular to sliding direction. The damage types characterised correspond well with the stages of damage observed for the galling wear mechanism in sheet metal stamping. The damage types 'Wear', 'Incipient galling', 'Transition to galling' match the initial asperity deformation and degrees of abrasion observed in sheet metal stamping prior to galling. The 'Wear' stage was visible but not quantifiable with laser microscopy on the test material, Everit 50 alloy. The 'incipient galling' damage stage, was described to be at the scale of existing surface asperities, with features being less than 1μm in size for the test material. The 'Transition to galling' stage was classified as features exceeding ½ R_y, or $> 2\mu m$ and $\leq 5\mu m$ in size for the test material. Finally, galling damage was classified as features greatly exceeding ½ R_y by at least an order of magnitude, or $\geq 10\mu m$ in size for the test material. Cross-sections of the damage stages exhibit the 'U' shaped gouge with raised shoulders that has been previously described, with the significant difference between the stages being scale. Seifert and Babu's [26] observations provide a numerical description of the difference between galling and abrasion damage that is typically observed in sheet metal stamping as a precursor to galling damage.
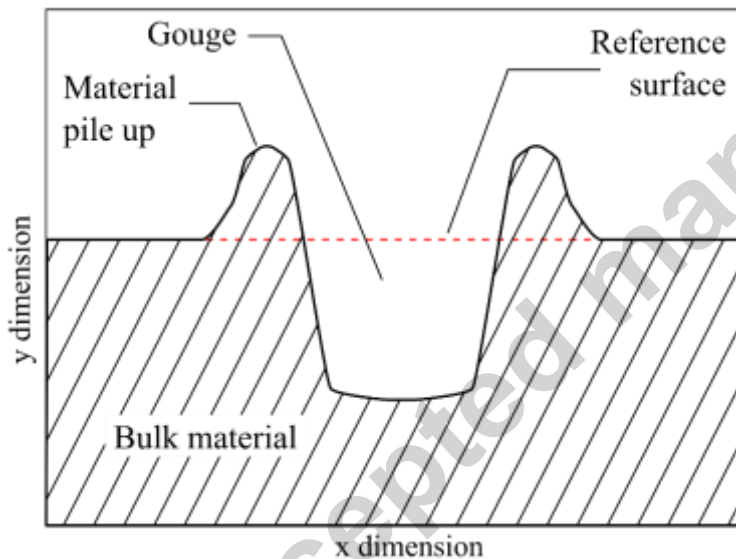

Figure 1: Typical simplified cross-section of abrasive or galling gouge, characterised by the material pile-up either side of the gouge in the surface.

2.2 Frequency analysis of surface profiles and Wavelet Transform

Engineering surfaces can be characterised by different spatial frequency or wavelength bandwidths. This is most evident with the common practice in surface metrology of using wavelength bandwidths to separate surface roughness, waviness, and form [36].

Characterising galling wear features in terms of spatial frequency allows for a targeted measure of galling wear severity. As discussed in section 2.1, FFT is one way to approach this characterisation, however, the associated loss of spatial information makes linking specific spatial frequencies to galling wear difficult. Wavelet Transform is a signal analysis technique that decomposes signals with localised wave-like functions, which represents signals in both the frequency domain and the spatial domain

simultaneously and, as such, provides a good representation of localised signal features [37]. Wavelet Transform has been used extensively to analyse and process 2D roughness profiles, often for the detection of discontinuities in surfaces [38–45]. However, Wavelet Transform has not been used for the characterisation and measurement of wear.

There are several wavelet functions or mother wavelets, $\psi(x)$, available for use in Wavelet Transform – examples can be seen in Figure 2. Numerous mother wavelet functions exist and some are likely to be better suited for galling wear characterisation than others.
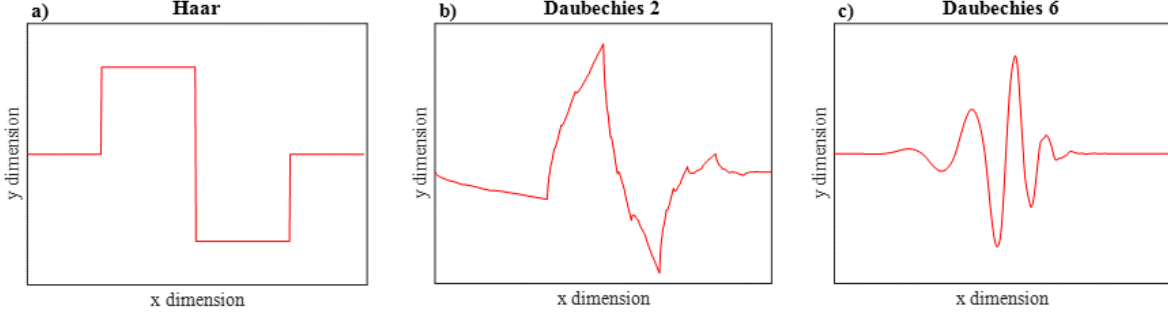

Figure 2: Example mother wavelet functions a) Haar wavelet, b) Daubechies 2, c) Daubechies 6.

The Discrete Wavelet Transform (DWT) is a common implementation of Wavelet Transform for practical applications using discrete data [46]. DWT decomposes a signal $f(x)$, where $-\infty \leq x \leq \infty$, by translating scaled copies of the mother wavelet, $\psi_{j,k}(x)$, across the signal and performing a convolution operation at each discrete translation step. Figure 3 shows the scaling and translation operations on the Daubechies 2 mother wavelet function. The wavelet base is defined as:

$$\psi_{j,k}(x) = 2^{j/2}\psi(2^j x - k) \tag{1}$$

Where j and k are integers, denoting the frequency or scale and space location or translation, respectively. The wavelet scaling function, $\phi_{j,k}(x)$, is defined as:

$$\phi_{j,k}(x) = 2^{j/2}\phi(2^j x - k) \tag{2}$$

In DWT the signal is broken-down into low pass approximation coefficients $c_j(k)$ and high pass detail coefficients $d_j(k)$, such that the wavelet expression of the signal is:

$$f(x) = \sum_k c_j(k)2^{j/2}\phi(2^j x - k) + \sum_k d_j(k)2^{j/2}\psi(2^j x - k) \tag{3}$$

Practically these coefficients can be determined using:

$$c_j(k) = \sum_k h(n)\, c_{j,k}(2k + n) \tag{4}$$

$$d_j(k) = \sum_k h_1(n)\, c_{j,k}(2k + n) \tag{5}$$

5

With $h(n)$ and $h_1(n)$ denoting quadrature mirror filters, a low and high-pass filter pair, where n is an integer in the sequence of discrete points of the input signal. The coefficients represent the level of correlation between the wavelet bases and the signal at each translation step. The approximation coefficients provide the low frequency component of the input signal and the detail coefficients capture the high frequency component.
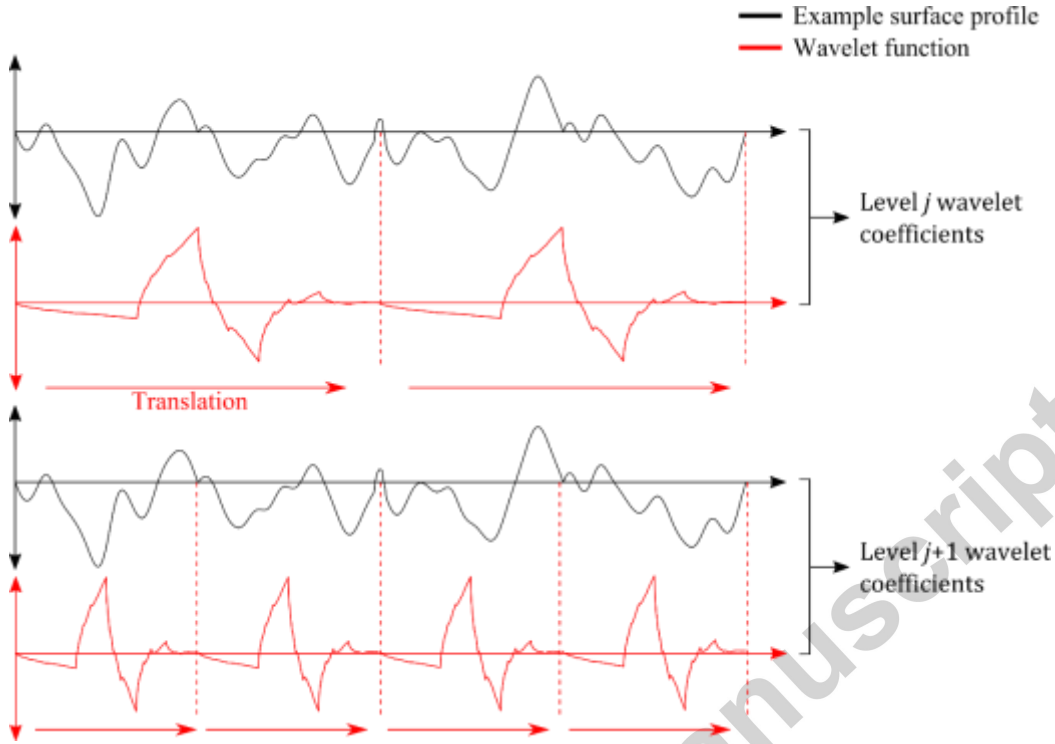

Figure 3: Schematic explanation of the Discrete Wavelet Transform operation, where the mother wavelet function is scaled and translated relative to the surface profile in order to calculate wavelet coefficients.

The multi-level decomposition DWT [47] iteratively applies Equation (4) and Equation (5) on the current approximation coefficients (Figure 4). At each level the wavelet function is scaled to provide coefficients that represent different wavelet frequency bandwidths.
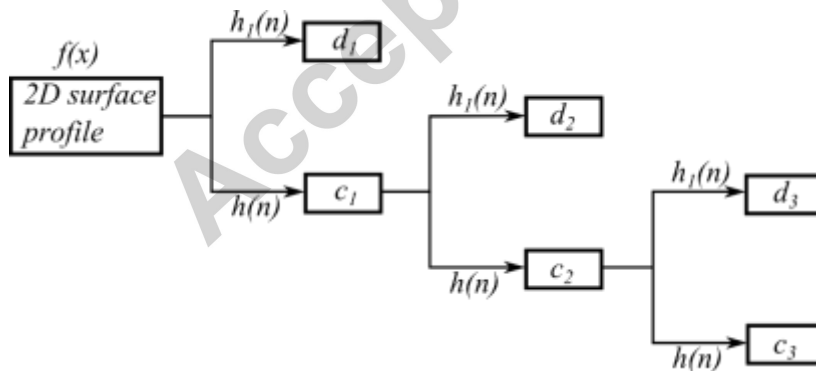

Figure 4: Multi-level DWT decomposition diagram, at each level detail and approximation coefficients are calculated and the decomposition is repeated on the approximation coefficients.

In sliding wear conditions, it has been shown that the abrasive damage preceding galling can be of similar depth as the existing surface asperities or roughness [9]. From this it has been inferred that wear features will be active in the same high frequency component of a surface profile as roughness. By

6

assessing detail coefficients from different levels of the multi-level DWT, it will be possible to isolate specific bandwidths that best characterise galling wear features.

3 Discrete Wavelet Transform for measuring galling wear severity

3.1 Surface Profile collection

The galling wear severity measurement method requires the collection of 2D surface profiles perpendicular to the sliding direction, or the direction of galling wear features. These profiles must capture the cross-section of the galling wear gouge tracks, see Figure 5. Transfer of material that leaves debris adhered to the wear surface or adhesive tear-out scars are two other wear features that are possible on galled formed part surfaces [5]. These features are localised in both sliding and perpendicular to sliding directions and so are difficult to capture with individual 2D profiles, therefore they will not be targeted in the presented methodology.
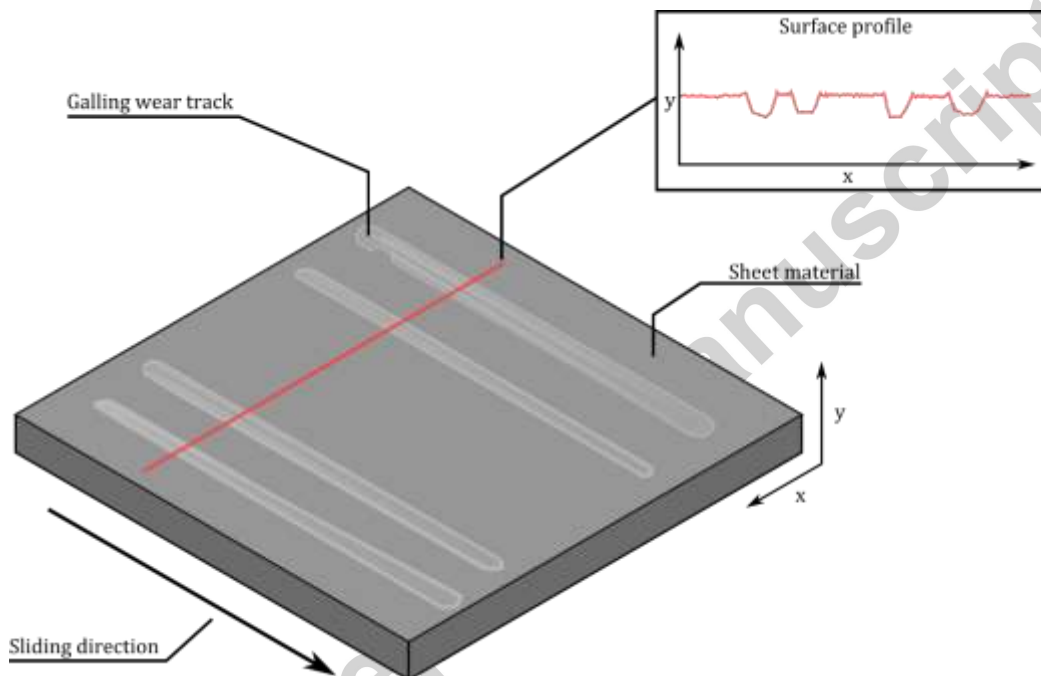

Figure 5: 2D surface profile collection schematic. The 2D profile is collected perpendicular to the sliding direction of the formed part in order to capture the cross-section of any galling wear gouges.

3.2 Mother wavelet selection

There are numerous mother wavelet functions available with Discrete Wavelet Transform decomposition, and each of these will provide varying results. Selecting an appropriate mother wavelet that matches the signal or galling wear feature is crucial for effectively characterising galling wear. Qualitative comparison between the signal and mother wavelet is a common method for selection in other applications such as power quality assessment and medical Electromyograms [48]. In these cases, the shape of the mother wavelet is compared visually to the feature of interest in the respective signals. Example mother wavelet functions of the Daubechies wavelet family and the Haar wavelet can be seen in Figure 2.

For assessing galling, the shape of the selected wavelet function must resemble the increase and sudden drop in the 2D profile that occurs due to material pile-up on the edges of the gouge, as shown in Figure 6a. The Daubechies 2 mother wavelet represents a close approximation of these features. A large

7

positive pulse immediately followed by a negative pulse corresponds well with the material build-up next to the wear gouge, as shown in Figure 6b. Because of these attributes the Daubechies 2 wavelet has been selected for analysis targeting galling wear and preceding damage in this study. Other galling wear features such as adhered material or adhesive pull-out scars may require selection of different mother wavelet functions for accurate measurement.
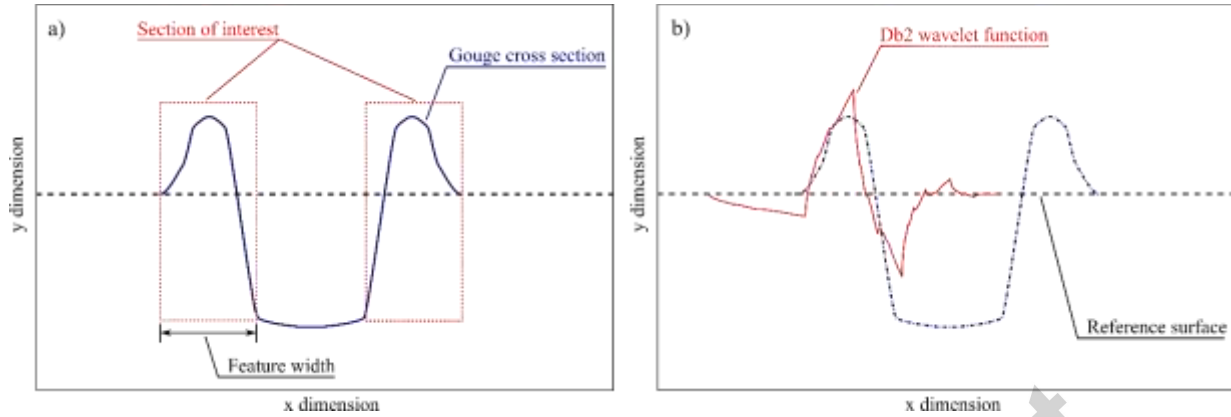

Figure 6: a) 2D profile galling wear cross-section features of interest. b) Selecting an appropriate mother wavelet function for galling wear feature of interest.

There are a number of quantitative measures available for the selection of mother wavelet function. Quantitative techniques require a representative signal, in this case a surface profile of galling wear damage. To supplement the use of qualitative selection, the Minimum description length (MDL) criterion has been applied to a surface profile collected from a wear damaged part formed in the case study presented in section 4. MDL criterion [49] is a quantitative technique that is commonly used in noise suppression and signal compression applications [48]. The MDL criterion determines the 'best' wavelet function by searching for the function that provides the most compact description of the data of interest. MDL was determined for the test surface profile (Die I part 14) using 51 wavelet functions from the MATLAB wavelet toolbox, and the 'db2' mother wavelet function was found to be in the top 10% as determined by MDL criterion.

3.3   Detail coefficient level selection

In order to quantify the severity of galling wear a detail level must be selected that has a wavelet frequency bandwidth that corresponds to the scale of the wear damage features. This can be achieved by examining example features from the relevant data set and by noting the scale and width at which those features exist, as shown for the example gouge cross-section in Figure 6a.

Once the width of the wear features has been determined, the appropriate detail coefficient level must be selected. The wavelet wavelength bandwidths of detail coefficient levels can be determined as a function of the sampling frequency f_s of the acquired surface profiles. Table 1 shows wavelet wavelength bandwidths of detail coefficients for a 6-level decomposition as a function of sampling frequency, and bandwidths for a sampling frequency of 1766 samples/mm. This sampling frequency and the selection of the detail coefficient level for the case study in this analysis will be described in Section 4.2.

8

Table 1: Discrete Wavelet Transform decomposition detail level wavelet frequency bandwidth ranges in terms of surface profile collection sampling frequency f_s.

Detail level	Wavelet wavelength bandwidth	Bandwidths for f_s
d_1	$2/f_s - 4/f_s$	1.13 – 2.27 μm
d_2	$4/f_s - 8/f_s$	2.27 – 4.53 μm
d_3	$8/f_s - 16/f_s$	4.53 – 9.06 μm
d_4	$16/f_s - 32/f_s$	9.06 – 18.12 μm
d_5	$32/f_s - 64/f_s$	18.12 – 36.24 μm
d_6	$64/f_s - 128/f_s$	36.24 – 72.48 μm

3.4 Detail coefficient calculation and wear severity quantification

Once the mother wavelet and the decomposition detail level are selected, the multi-level wavelet decomposition of the surface profile is completed and the specified detail coefficients determined according to Equation (4) and Equation (5). Large detail coefficient values indicate a high likelihood of a distinct wear feature of the corresponding scale. The detail coefficients also provide the relative location in the profile of the wear features.

3.5 DWT wear severity parameter

The detail coefficients can be processed to provide a single galling wear severity value, W_{DWT}, by taking the mean of absolute values of the detail coefficients, Equation (6). Where N is the number of coefficients.

$$W_{DWT} = \sum |d_j|/N \qquad (6)$$

The individual W_{DWT} values can be compared with values from the same mother wavelet function and wavelet frequency bandwidth, but cannot be directly compared to values determined under different DWT conditions.

4 Case study

4.1 Experimental setup

A case study has been conducted to demonstrate the Discrete Wavelet Transform galling wear methodology. A series of channel parts have been formed until galling wear was visually observed on the dies and testing was ceased. The proposed DWT galling wear severity parameter (W_{DWT}, see Equation (6)) was calculated from 2D profile measurements of the part surfaces and compared to visual rankings. Visual rankings are used as the reference measurement, because these are the current standard for evaluation and quantification of galling wear severity, as described in Section 2.1.

4.1.1 Channel forming operation

Wear test samples or parts were formed using the channel forming test shown in Figure 7. The channel forming process was conducted on an Erichsen Universal Sheet Metal Testing Machine (Model 145-60) with the geometry and main process conditions summarised in Table 2. The process is designed to allow for close replication of conditions seen in the forming of automotive sheet metal components. The tooling geometry features two symmetrical removable die radius inserts (Die I and Die II), that are designed for easy removal. The high contact pressures on these die inserts result in wear damage being

localised on the inserts and counter surface of the channel part sidewalls. Further details of the experimental setup can be found in [50].
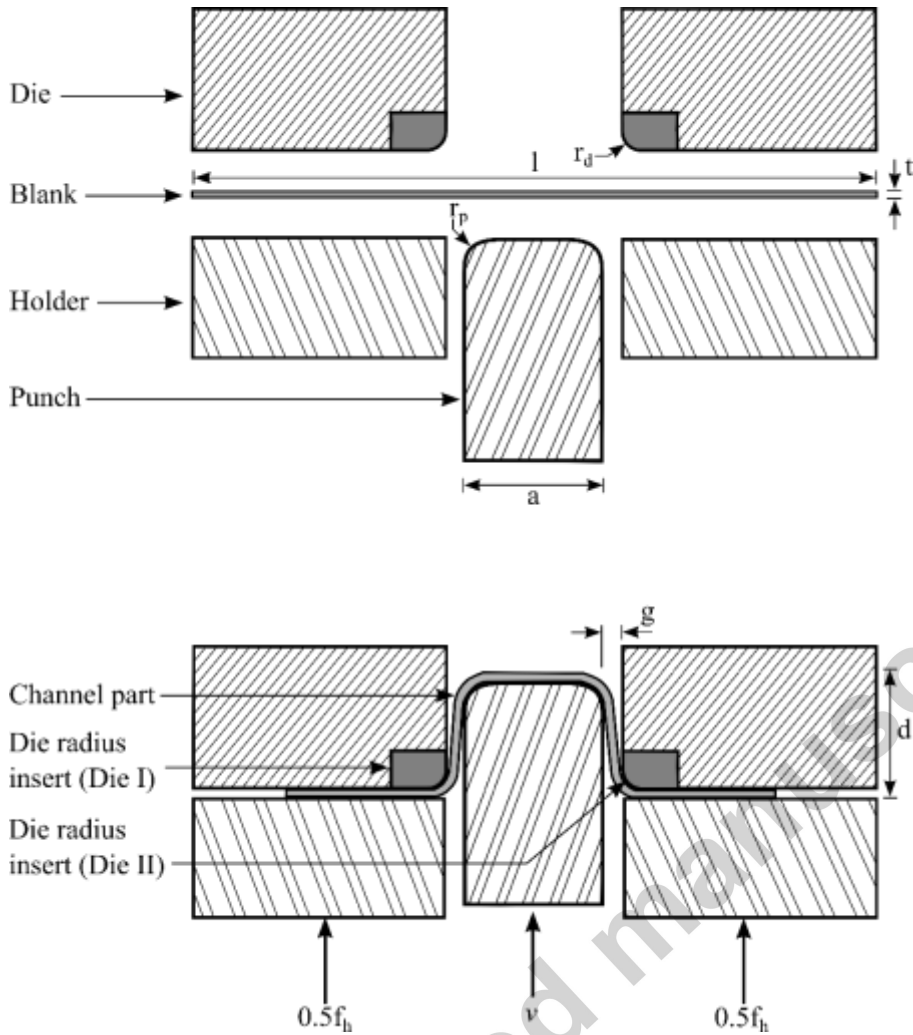

Figure 7: Schematic of the channel forming process.

Table 2: Channel forming operation process variables.

Channel forming operation process variables		
Punch width, a		40 mm
Draw depth, d		50 mm
Die-to-punch gap, g		2.1 mm
Blank length, l		150 mm
Blank holder force, f_h		20 kN
Die radius, r_d		5 mm
Punch corner radius, r_p		5 mm
Blank thickness, t		2 mm
Blank width		19.5 mm
Tool-to-sheet clearance		0.1 mm
Punch speed, v		1.5 mm/s
Die radius roughness	Sliding direction Ra	0.066 μm
	Transverse direction Ra	0.164 μm
Die material		AISI D2 tool steel
Blank material		Uncoated DP600
Die hardness		60 HRC

Number of parts formed	14
Number of die wear samples	28

4.1.2 Surface characterisation

3D surface scans were collected for each part sidewall using 3D focus-variation scanning microscopy (Alicona Infinite Focus). The location of the 3D surface profilometry scans and the visual assessment region are shown in Figure 8. Aggregate 2D surface profiles perpendicular to the sliding direction of forming were then collected from the centre of these 3D surface scans, and calculated using the mean of 70 adjacent profiles spanning a region of width 50μm (Figure 8). This ensured that sliding direction wear tracks were captured by the profiles and asperity noise was minimised. The sampling frequency or sample spacing of the 2D surface profiles was determined by the resolution of the 3D surface scans. For this study, the sampling frequency was 1766 samples/mm.

For comparison, a number of roughness and surface texture parameters were determined for the collected 2D profiles and 3D surface scans – see Table 3. The Galling Severity Index [34] is the only parameter directly targeted at galling quantification and requires the use of a reference unworn surface profile. The first part sidewall for each die were used as reference surfaces. A number of other 3D texture parameters and 2D surface profile parameter were also assessed, including: maximum valley depth (R_v), maximum peak height (R_p), root mean square of slope (R_{dq}), average height of area (S_a), and root mean square of gradient (S_{dq}). R_{dq} has been linked to tool wear in machining [51] and performed well in initial measurements, and so was included in this comparison.

Table 3: Alternate wear measures.

Parameter	Description
R_a	Average roughness of profile
R_z	Mean peak to valley height of roughness profile
R_y	Maximum peak to valley height of roughness profile
R_p	Maximum peak height
R_v	Maximum valley depth
R_{dq}	Root mean square of slope
GSI	Galling Severity Index
S_{pk}	Mean peak height above core roughness
S_k	Height of core roughness
S_{vk}	Mean depth of valleys below core roughness
S_a	Average height of area
S_{dq}	Root mean square of gradient

4.1.3 Visual wear assessment and ranking

Categorical visual rating scales of galling and wear damage have been used to provide subjective quantitative outputs of the visual assessment of galling wear damage on strip drawn samples [7], cylindrical cups [20], and ASTM G 98 and G 196 test specimens [27]. A tailored visual wear damage severity rating scale has been used to assess formed parts. The tailored visual wear damage severity scale has been developed to ease with assessment of the channel parts formed in this case study and is shown in Table 4. Images of the sidewalls were assessed by 9 assessors experience with sheet metal forming, including the authors, and a median rating for each part was determined. The channel forming operation was ceased when galling damage was observed on the die, with the counter surface on the formed parts exhibiting abrasive damage. The visual ranking score ranges from 0-5 in value; where a score of 0 is allocated if no wear is observed and 5 is allocated if severe damage is judged, as seen in Table 4. The issues with the application of numerical rankings to visual assessment of large worn surfaces have been discussed in Section 2.1. Considering these issues and to improve the accuracy of the rankings and the ease by which they can be applied, only the immediate wear region where sliding

11

contact begins was assessed on each wear test sample, as seen in Figure 8. The assessment regions were considered to start 2 mm in from the edge of the parts to ignore edge effects and were divided into two equal regions perpendicular to the sliding direction such that each wear test sample was assigned 2 rankings. The width of the parts was 20 mm, which meant that wear development could occur at localised regions perpendicular to the sliding direction and therefore this division was conducted to improve ranking accuracy. A combined damage severity rating was then calculated for each wear test sample by summing the ratings assigned to the two regions to give a combined damage severity rating out of 10. The resulting visual assessment rankings from the 9 assessors for the two dies are summarised with box plots in Figure 9, with the red line showing the median ranking for each part sidewall. Outliers are defined as responses greater than $Q_3 + 1.5 * IQR$ and less than $Q_1 - 1.5 * IQR$, where IQR denotes the interquartile range and Q_1 and Q_3 represent the 25th and 75th percentile of the response data for each part sidewall respectively. Example aggregate median damage severity ratings are shown with the images of the corresponding part sidewalls in Figure 10.
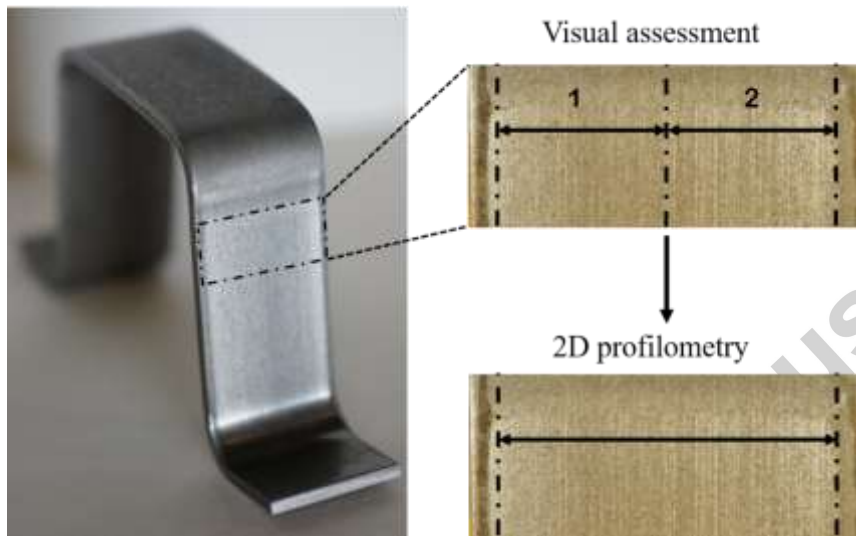

Figure 8: Part sidewall assessment division. Only the section at the initiation of steady state contact is considered and is subdivided into sections 1 and 2 for numerical ranking of galling wear severity. This same region is scanned using focus-variation scanning microscopy and a 2D aggregate profile is collected for the wear severity measurement.

Table 4: Visual assessment wear damage rankings.

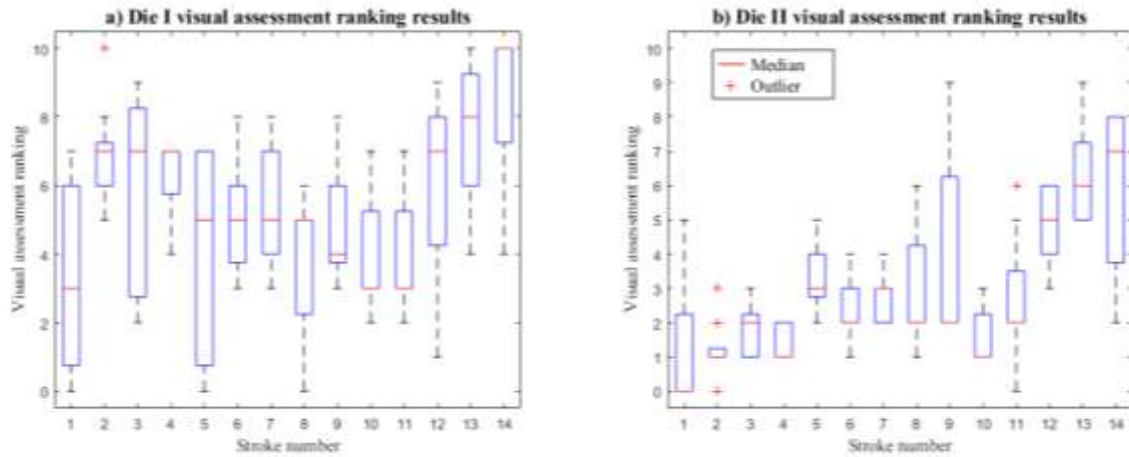| Wear ranking	Definition
0	Smooth, no apparent wear
1	Very slight scratching
2	Mild scratching apparent
3	Obvious scratching in small proportion of side wall
4	Obvious scratching on significant proportion of sidewall half
5	Obvious scratching on entire sidewall half or very severe scratching

12

Figure 9: Box plots depicting part sidewall visual assessment rankings from 9 assessors who have ranked each of the 28 part sidewalls according to section 4.1.3. Red lines depict the median visual assessment ranking for each part sidewall, + represent outlier ranking values for individual part sidewalls, whiskers represent the range of the ranking values and the blue boxes depict the range of quartiles 1 to 3. a) Die I results, b) Die II results.

Die II Part 1	Die I part 12	Die I part 14
Median ranking = 0	Median ranking = 7	Median ranking = 10

Figure 10: Examples of the numerical wear severity rankings for three wear test samples.

4.2   Detail coefficient level selection

In order to select an appropriate decomposition detail level, a number of example galling wear gouges were isolated in the captured 2D surface profiles from Die I stroke numbers 4 and 14 and Die II stroke numbers 13 and 14. In these 2D surface profiles the edge transitions of the wear gouges, seen in Figure 6a, were measured and found to occur over an average distance of 18μm. One example galling wear gouge and edge transition measurement can be seen in Figure 11.
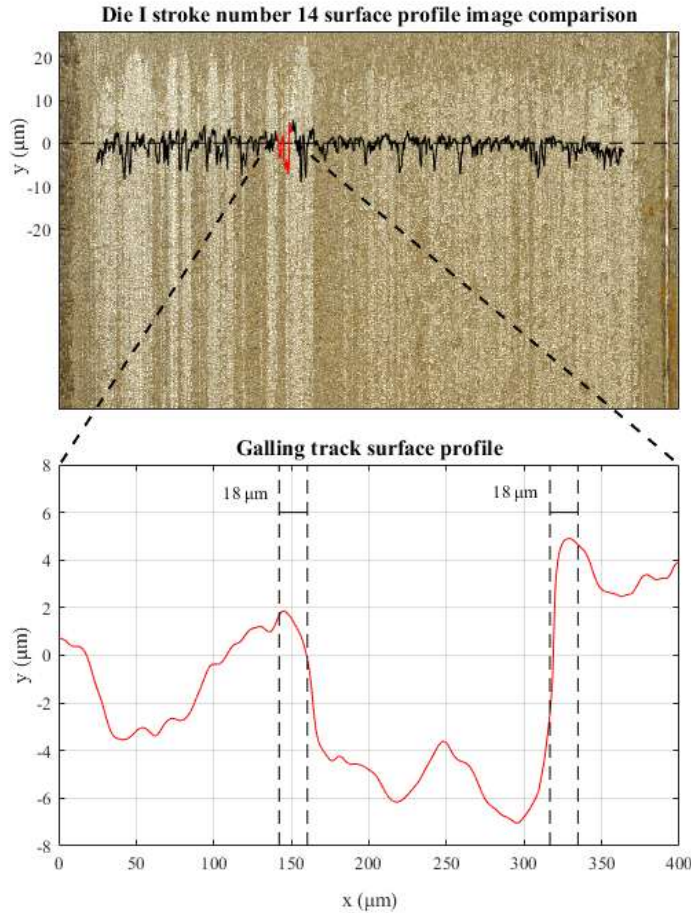
13

Figure 11: An example galling wear gouge track isolated from the 2D surface profile. Key gouge track edge transitions present at 150μm and 325μm are measured to determine the appropriate Discrete Wavelet Transform decomposition detail level.

The sampling rate at which the profiles were collected was 1766 samples per mm and so the detail levels correspond to the wavelength bandwidths seen in Table 1. Detail level 4 (d_4) approximately covers the 18μm gouge edge transition and so has been selected as the output detail level.

4.3   Results and analysis

4.3.1   DWT detail coefficients

A DWT multi-level decomposition was performed on the collected roughness profiles using Mathwork's Matlab Wavelet Toolbox. The resultant Daubechies 2 level 4 detail coefficients (d_4), Equation (5), were overlaid on images of corresponding wear test samples to qualitatively check the correlation between the detail coefficients and the visual observation of scratches on the sidewalls of the parts (as shown in Figure 12). It is evident that there is very good qualitative correlation (both in terms of the location and magnitude) between the detail coefficient parameter and the visual severity of the wear damage.
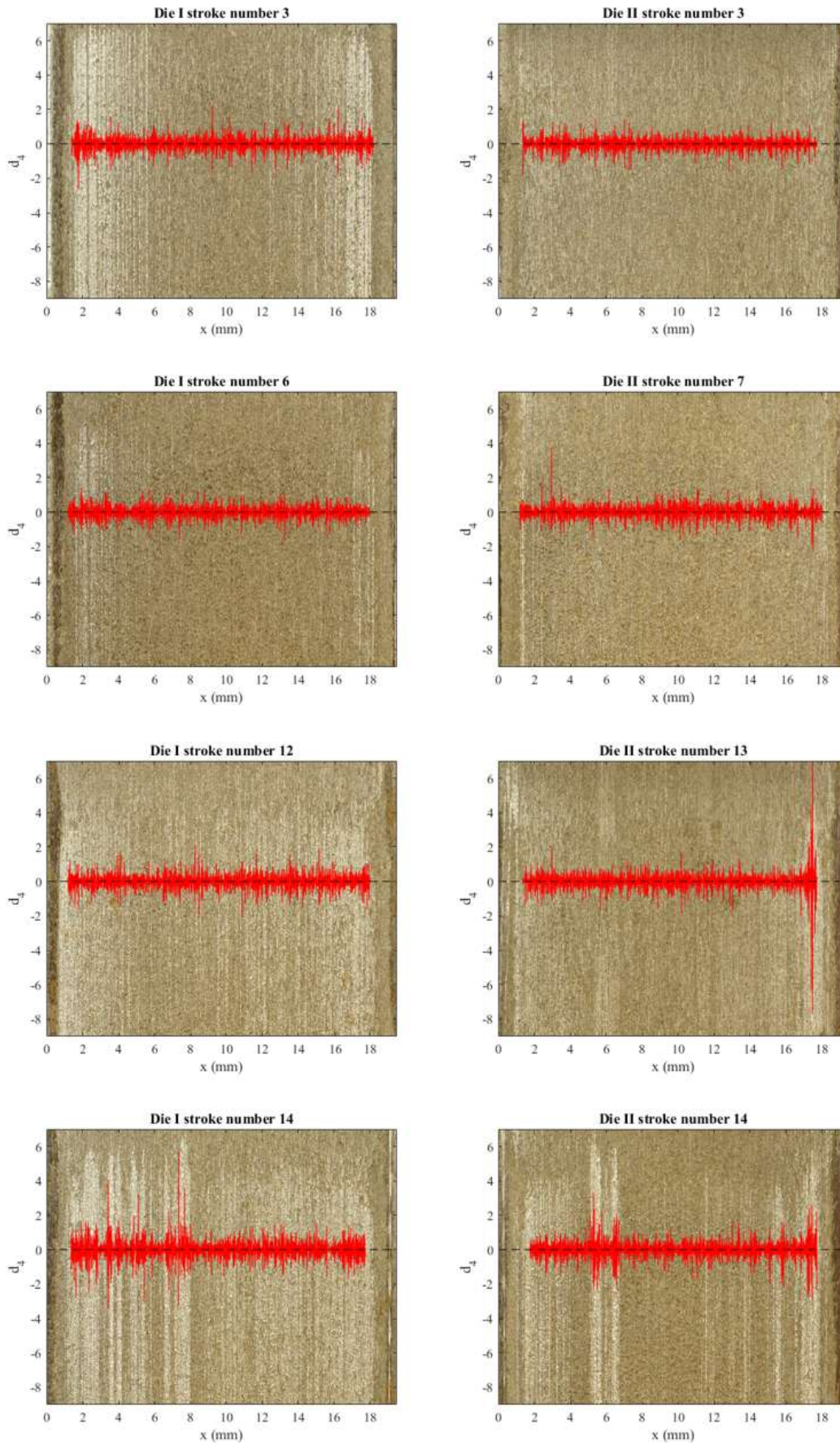
Figure 12: Detail coefficient (Daubechies 2 detail level 4) overlaid on wear test samples images, demonstrating the detail coefficient response to galling wear features.

4.3.2 Wear parameters

The progression of each galling wear measurement parameter or surface roughness parameter for both dies can be seen in Figure 13. As discussed, the visual assessment ranking (shown in Figure 13a) is the baseline measurement of galling wear for the parts. W_{DWT} values determined for a different wavelet function (Figure 13e) and different wavelet frequency bandwidth (Figure 13d) have been included as a comparison for a non-optimised DWT process. The values calculated with the Haar wavelet at detail level 4 (Figure 13e) and Daubechies 2 wavelet at detail level 6 (Figure 13d) represent values determined with sub-optimal wavelet function and wavelet frequency bandwidth respectively. Figure 13c also shows the calculated *GSI* parameter values, which is the only other galling wear targeted parameter. The best performing 'traditional' surface roughness-based parameter, R_{dq}, is shown in Figure 13f. Finally, R_a, S$_{vk}$, and S$_{pk}$ have been included as representative examples of other traditional roughness and texture parameters.
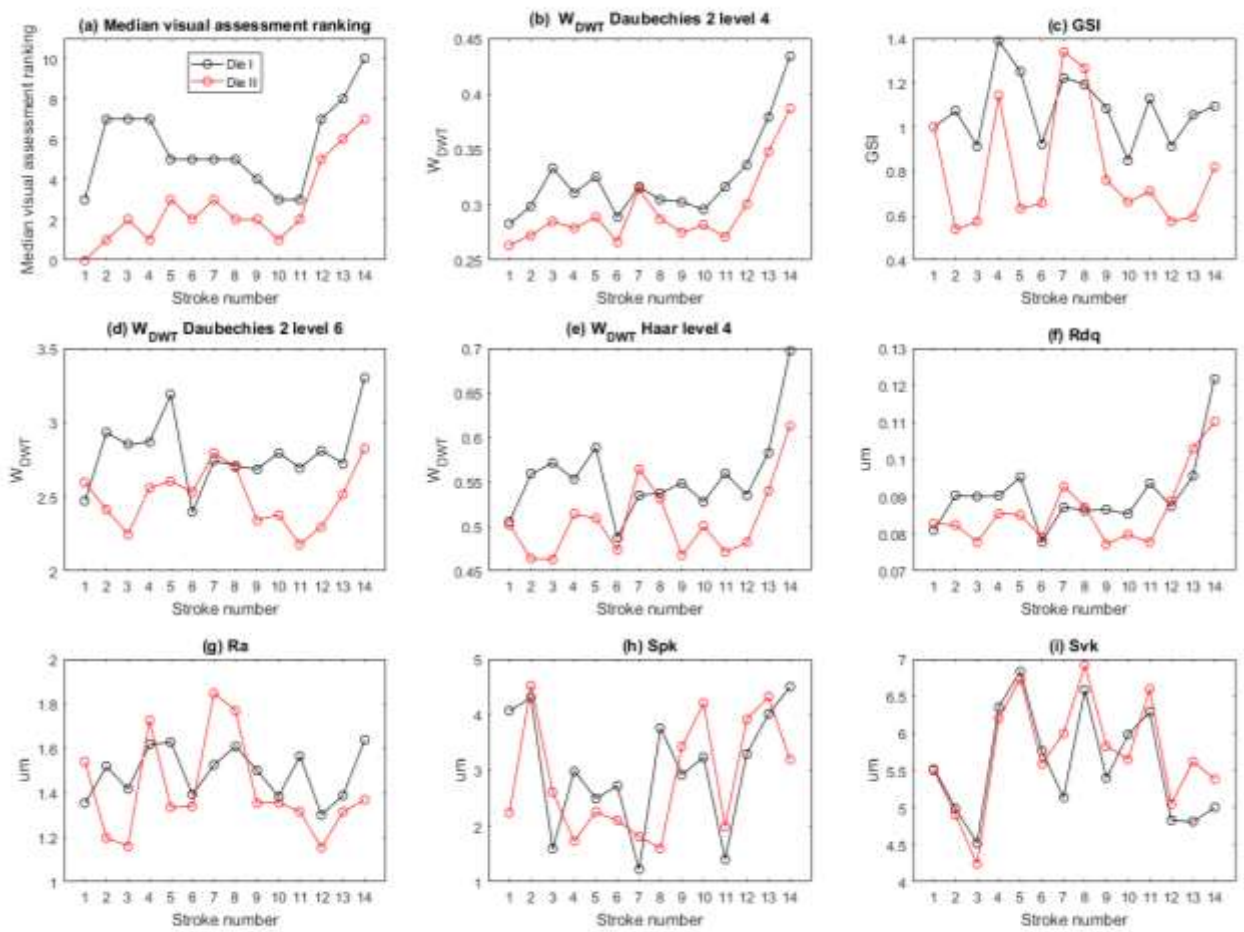
Figure 13: Assessed galling wear measurements for each die insert with stroke number, showing the progression of each parameter over the course of the wear trials for both dies.

The correlation between each of the wear measures and the visual assessment ranking was then measured using Spearman's rank Correlation Coefficients, r_s [52], using a total of 28 data points for each case. Spearman's rank correlation provides a measure of the rank correlation between two variables and is suitable for application to ordinal data, like the visual assessment rankings collected in this study. The performance of the parameters in Table 3 was measured against numerical rankings of

16

galling wear severity based on visual assessment, which is the standard for assessment of galling wear severity [23,24]. Correlation coefficient and *p*-values for correlation with visual assessment ranking values for the parameters listed in Table 3 can be seen in Table 5. W_{DWT} was found to have a significant and highest correlation of $r_s = 0.8688$ with the visual assessment ranking.

Table 5: Spearman's rank correlation value for wear measures with median visual assessment ranking.

Median visual assessment ranking correlation results		
Parameter	Correlation coefficient r_s	*p*-value
W_{DWT} Daubechies 2 level 4 (optimised)	0.8688	2.04E-09
W_{DWT} Haar level 4 (not optimised)	0.6612	1.28E-04
W_{DWT} Daubechies 2 level 6 (not optimised)	0.7293	1.07E-05
R_{dq}	0.7245	1.30E-05
GSI	0.2567	0.1873
R_a	0.1152	0.5595
R_z	0.0572	0.7731
R_y	0.0975	0.6277
R_p	0.2807	0.1479
R_v	-0.0498	0.8012
S_{pk}	0.2664	0.1707
S_k	0.0349	0.8601
S_{vk}	-0.3212	0.0956
S_a	-0.0642	0.7454
S_{dq}	-0.2315	0.2360

5 Discussion

Summarising the results, it can be stated that the presented method maintains the accuracy of visual assessment, but shows greater reliability when regarding the limitations and variability of visual assessment. Visual assessment is a subjective process that is challenging to apply to large surface areas, and does not always lead to repeatable measurements of galling wear. The significant variability of visual assessment is demonstrated with the respondent assessment results shown in Figure 9. Numerical ranking provides a quantifiable output for visual assessment and median values address variability, however the subjective nature of the method and the difficulties with repeatability and application over large surface areas remain.

The DWT detail coefficients capture the important information about the wear features, and W_{DWT} converts the detail coefficient information into a form that is suitable for direct comparison to visual assessment rankings. However, condensing the wear information from the detail coefficients to the single W_{DWT} parameter results in the loss of spatial information. Therefore, the W_{DWT} values should be considered as one component in the presented methodology for measuring and characterising galling wear, rather than the definitive output.

There is a level of noise present in the detail coefficients that is due to low levels of wavelet correlation with other surface features. This is an issue that is exacerbated when using single 2D surface profiles as opposed to aggregated 2D surface profiles. While some noise still exists, it is apparent from the detail coefficient image overlay, Figure 12, that the wear features produce the dominant detail coefficient values. Utilising aggregate 2D surface profiles minimises this noise by reducing the prominence of non-wear related surface asperities and pitting. Figure 12 demonstrates that the galling wear features are well characterised by DWT detail coefficients for Daubechies 2 of wavelength 9.09 - 18.2μm, with the highest values of the detail coefficients at the galling wear features locations. The 9.09 - 18.2μm

17

wavelength bandwidth that is associated with detail level 4 in this study is shown to cover the same spatial range as galling wear features in Figure 11.

The root mean square slope of the profile, R_{dq}, was found to have a significant correlation with visual assessment rankings; however, this correlation was not as strong as that found with optimised W_{DWT} values. R_{dq} gives a measure of variability of the surface and has been linked to wear in machining tools and has been used for assessing reflectivity and wettability of surfaces [51,53]. It follows that this parameter will respond to the sudden drops below the bulk material level in the 2D profiles that are associated with galling related wear features (e.g. see Figure 1 and Figure 11). However, R_{dq} is likely to be more susceptible to the base surface roughness than the DWT methodology presented in this study. GSI is the only other parameter that is specifically targeted at galling wear measurement, and has been shown to be effective when measuring severely galled parts [34]. GSI performed poorly when compared to visual assessment ranking and W_{DWT} for the parts collected in the conducted case study. The collected parts exhibited primarily abrasive damage features that precede galling that are likely to be less prominent and less frequent in their occurrence than any features seen on parts exhibiting severe galling damage. By converting the profiles into the frequency domain and averaging the response, it is likely that the smaller scale wear features, that are an indication of galling severity, are lost in the response of the general surface roughness.

The DWT methodology provides a targeted, repeatable and non-subjective measure of galling wear severity in sheet metal stamping. Of the parameters tested, the presented optimised W_{DWT} value was found to correlate best with median visual assessment rankings, with a correlation coefficient value of $r_s = 0.8688$ and p-value of 2.04E-09 (see Table 5). The methodology is appropriate for sheet metal forming tests that focus on galling wear in industrial style conditions where 2D profiles can be collected perpendicular to the sliding direction. The method allows the quantification of multiple localised galling wear features over large surface areas, as opposed to fixed single tracks that are often studied in experimental wear trials. Therefore, the method will also be applicable to other sliding wear experiments used for galling analysis, such as bending-under-tension and slider-on-sheet tests. Galling wear progression can occur over the course of individual strokes, resulting in varying levels of galling wear severity on a single part. The presented methodology is based on 2D profilometry, and so the resultant measure is dependent upon the surface profile location. Selecting a measurement location that corresponds to later in the stroke or taking multiple measurements will help to ensure an accurate measure of the wear severity is captured.

The presented methodology may also be applicable for identifying other localised wear features on formed sheet metal surfaces, such as fatigue cracks and graphic nodule pull-out that have been observed in cast iron dies [5,54]. Both of these features are localised, which makes DWT appropriate for their characterisation. However, as per the methodology, appropriate mother wavelet functions and wavelength bandwidths need to be identified, as highlighted by the lower correlation coefficients observed for the non-optimised W_{DWT} values included in the case study (see Table 5).

Future work should also focus on numerically determining the transition points between progressive stages of wear damage using the presented methodology. The difference stages of wear damage development feature similar cross-sectional geometries but at varying scales. This opens up the possibility of focusing on specific wavelength bandwidths or detail coefficient levels in order to distinguish between the before mentioned stages. Such an approach would be dependent upon the chosen material and sampling frequencies of the surface profile. Tracking the progression of localised wear damage and making comparisons to visual characterisations would also be required in order to develop the corresponding transition values, for both detail coefficients and W_{DWT} values. With these transition points determined, the DWT methodology could be a useful addition to standard galling resistance tests such as ASTM G98 and G196. In these tests galling damage is visually identified and is subject to the variability of visual assessment. The presented methodology could be used to measure for

the presence of galling damage by collecting surface profiles perpendicular to the sliding direction or along the radius of the test button, and monitoring detail coefficient values.

6 Conclusions

A new methodology for measuring and quantifying galling wear severity based on Discrete Wavelet Transform of 2D profiles has been presented. The localised wavelet functions that are used in Wavelet Transform are ideal for detecting the wear features and correlate well with the shape of galling wear features such that it is possible to separate the wear from surface roughness. The DWT detail coefficients were optimised for galling wear measurement according to the presented methodology. It was shown that the DWT detail coefficients correlate well with the position and severity of the damage associated with galling wear on the part sidewalls observed via visual inspection and photography. Since visual inspection is the current standard for galling assessment for many manufacturing processes – including sheet metal stamping – the study demonstrates the ability of the method to measure localised wear features associated with galling.

The new DWT galling wear severity parameter, W_{DWT}, was proposed based on the calculated DWT detail coefficients. The W_{DWT} parameter was found to correlate well with visual assessment rankings (r_s = 0.8688). As demonstrated via a sheet metal stamping case study, W_{DWT} significantly outperformed existing galling, roughness and texture parameters that are commonly used as a measure of wear or galling severity. Hence, W_{DWT} provides an accurate quantifiable measure of galling wear severity, via measurement of the workpiece (i.e. part) surfaces and not the tool surfaces. Additionally, the DWT methodology presented in this study is simple to implement in industrial-style sheet metal stamping trials as well as laboratory-based galling experiments. Simple and accurate methods for measurement and characterisation of galling wear in industrial situations are crucial for further investigation into, and development of, wear monitoring and detection systems. The results also have broader applicability for further study on galling wear and its prevention. Therefore, this study is an important contribution towards addressing galling wear in industrial sheet metal stamping, which continues to be a significant challenge to industry.

7 Acknowledgements

8 References

[1] Zhou, R., AlAli, I., Cao, J., Wang, Q., and Xia, Z. C., 2009, Experimental Analysis of Die Wear in Sheet Metal Forming, Warrendale, PA.

[2] Jantunen, E., 2002, "A summary of methods applied to tool condition monitoring in drilling," Int. J. Mach. Tools Manuf., **42**(9), pp. 997–1010.

[3] Schedin, E., and Lehtinen, B., 1993, "Galling mechanisms in lubricated systems: A study of sheet metal forming," Wear, **170**(1), pp. 119–130.

[4] Schedin, E., 1994, "Galling mechanisms in sheet forming operations," Wear, **179**(1), pp. 123–128.

[5] Gåård, A., Krakhmalev, P., and Bergström, J., 2008, "Wear mechanisms in deep drawing of carbon steel – correlation to laboratory testing," Tribotest, **14**(1), pp. 1–9.

[6] ASTM Standard G40-15, 2015, Standard Terminology Relating to Wear and Erosion, West

Conshohocken, PA.

[7] Andreasen, J. L., Bay, N., and De Chiffre, L., 1998, "Quantification of galling in sheet metal forming by surface topography characterisation," Int. J. Mach. Tools Manuf., **38**(5–6), pp. 503–510.

[8] Karlsson, P., Gåård, A., Krakhmalev, P., and Bergström, J., 2012, "Galling resistance and wear mechanisms for cold-work tool steels in lubricated sliding against high strength stainless steel sheets," Wear, **286**–**287**, pp. 92–97.

[9] Gåård, A., Krakhmalev, P., and Bergström, J., 2009, "Influence of tool steel microstructure on origin of galling initiation and wear mechanisms under dry sliding against a carbon steel sheet," Wear, **267**(1), pp. 387–393.

[10] van der Heide, E., Huis in 't Veld, A. J., and Schipper, D. J., 2001, "The effect of lubricant selection on galling in a model wear test," Wear, **251**(1–12), pp. 973–979.

[11] Galakhar, A. S., Gates, J. D., Daniel, W. J. T., and Meehan, P. A., 2011, "Adhesive tool wear in the cold roll forming process," Wear, **271**(11–12), pp. 2728–2745.

[12] Groche, P., Moeller, N., Hoffmann, H., and Suh, J., 2011, "Influence of gliding speed and contact pressure on the wear of forming tools," Wear, **271**(9), pp. 2570–2578.

[13] Wang, C., Chen, J., Xia, Z. C., and Ren, F., 2013, "Die wear prediction by defining three-stage coefficient K for AHSS sheet metal forming process," Int. J. Adv. Manuf. Technol., **69**(1–4), pp. 797–803.

[14] Pujante, J., Pelcastre, L., Vilaseca, M., Casellas, D., and Prakash, B., 2013, "Investigations into wear and galling mechanism of aluminium alloy-tool steel tribopair at different temperatures," Wear, **308**(1–2), pp. 193–198.

[15] Swanson, P. A., Ives, L. K., Whitenton, E. P., and Peterson, M. B., 1988, "A study of the galling of two steels using two test methods," Wear, **122**(2), pp. 207–223.

[16] Christiansen, S., and De Chiffre, L., 1997, "Topographic Characterization of Progressive Wear on Deep Drawing Dies," Tribol. Trans., **40**(2), pp. 346–352.

[17] Skåre, T., and Krantz, F., 2003, "Wear and frictional behaviour of high strength steel in stamping monitored by acoustic emission technique," Wear, **255**(7–12), pp. 1471–1479.

[18] Podgornik, B., Hogmark, S., and Pezdirnik, J., 2004, "Comparison between different test methods for evaluation of galling properties of surface engineered tool surfaces," Wear, **257**(7–8), pp. 843–851.

[19] Shaffer, S. J., and Rogers, M. J., 2007, "Tribological performance of various coatings in unlubricated sliding for use in small arms action components—A case study," Wear, **263**(7–12), pp. 1281–1290.

[20] Olsson, D. D., Bay, N., and Andreasen, J. L., 2010, "A quantitative lubricant test for deep drawing," Int. J. Surf. Sci. Eng., **4**(1), pp. 2–12.

[21] Ubhayaratne, I., Pereira, M. P., Xiang, Y., and Rolfe, B. F., 2017, "Audio signal analysis for tool wear monitoring in sheet metal stamping," Mech. Syst. Signal Process., **85**, pp. 809–826.

[22] Smith, D. A., 2001, Die maintenance handbook, Society of Manufacturing Engineers, Dearborn, MI.

[23] ASTM Standard G196-08, 2016, Standard Test Method for Galling Resistance of Material Couples, West Conshohocken, PA.

[24] ASTM Standard G98-02, 2009, Standard Test Method for Galling Resistance of Materials, West Conshohocken, PA.

[25] Hummel, S. R., 2011, "Elements to Improve Galling Resistance Test Results Using the ASTM G98 Method," J. Test. Eval., **39**(3), p. 103214.

[26] Siefert, J. A., and Babu, S. S., 2014, "Experimental observations of wear in specimens tested to ASTM G98," Wear, **320**, pp. 111–119.

[27] Budinski, K. G., and Budinski, S. T., 2015, "Interpretation of galling tests," Wear, **332**, pp. 1185–1192.

[28] Fildes, J. M., Meyers, S. J., Mulligan, C. P., and Kilaparti, R., 2013, "Evaluation of the wear and abrasion resistance of hard coatings by ball-on-three-disk test methods—A case study," Wear, **302**(1), pp. 1040–1049.

[29] Taşan, Y. C., de Rooij, M. B., and Schipper, D. J., 2005, "Measurement of wear on asperity level using image-processing techniques," Wear, **258**(1), pp. 83–91.

[30] Archard, J. F., 1953, "Contact and rubbing of flat surfaces," J. Appl. Phys., **24**(8), pp. 981–988.

[31] Kennedy, D. ., and Hashmi, M. S. ., 1998, "Methods of wear testing for advanced surface coatings and bulk materials," J. Mater. Process. Technol., **77**(1–3), pp. 246–253.

[32] Bhushan, B., 2002, Introduction to Tribology, John Wiley & Sons, New York.

[33] Yost, F. G., 1983, "Two profilometric measurements of wear," Wear, **92**(1), pp. 135–142.

[34] Vermeiden, M., and Hobleke, H., 2003, "Functionality and Characterisation of Textured Sheet Steel Products," L. Blunt, and X. Jiang, eds., Kogan Page Science, Oxford, pp. 249–305.

[35] Varjoranta, T., Hirvonen, J., and Anttila, A., 1981, "Measuring the wear of nitrogen-implanted steel," Thin Solid Films, **75**(3), pp. 241–245.

[36] Raja, J., Muralikrishnan, B., and Fu, S., 2002, "Recent advances in separation of roughness, waviness and form," Precis. Eng., **26**(2), pp. 222–235.

[37] Mallat, S. G., 2009, A wavelet tour of signal processing : the Sparse way, Elsevier /Academic Press.

[38] Lee, S.-H., Zahouani, H., Caterini, R., and Mathia, T. G., 1998, "Morphological characterisation of engineered surfaces by wavelet transform," Int. J. Mach. Tools Manuf., **38**(5), pp. 581–589.

[39] Wei, L., Fwa, T. F., and Zhe, Z., 2005, "Wavelet Analysis and Interpretation of Road Roughness," J. Transp. Eng., **131**(2), pp. 120–130.

[40] Papagiannakis, A. T., Zelelew, H. M., and Muhunthan, B., 2007, "A wavelet interpretation of vehicle-pavement interaction," Int. J. Pavement Eng., **8**(3), pp. 245–252.

[41] Fu, S., Liu, X., Muralikrishnan, B., and Raja, J., 2001, "Wavelet Analysis with Different Wavelet Bases for Engineering Surfaces," Proc. 16th Annu. Meet. Amer. Soc. Precis. Eng., **125**(November), pp. 249–252.

[42] Josso, B., Burton, D. R., and Lalor, M. J., 2002, "Frequency normalised wavelet transform for surface roughness analysis and characterisation," Wear, **252**(5), pp. 491–500.

[43] Rackov, D. M., Popovic, M. V., and Mojsilovic, A., 2000, "On the selection of an optimal wavelet basis for texture characterization," IEEE Trans. Image Process., **9**(12), pp. 2043–2050.

[44] Lingadurai, K., and Shunmugam, M. S., 2006, "Metrological characteristics of wavelet filter used for engineering surfaces," Measurement, **39**(7), pp. 575–584.

[45] Dutta, S., Pal, S. K., and Sen, R., 2016, "Progressive tool flank wear monitoring by applying discrete wavelet transform on turned surface images," Measurement, **77**, pp. 388–401.

[46] Burrus, C. S., Gopinath, R. A., and Guo, H., 1998, Introduction to wavelets and wavelet

transforms : a primer, Prentice Hall, Upper Saddle River, NJ.

[47]   Mallat, S. G., 1989, "A theory for multiresolution signal decomposition: the wavelet representation," IEEE Trans. Pattern Anal. Mach. Intell., **11**(7), pp. 674–693.

[48]   Ngui, W. K., Leong, M. S., Hee, L. M., and Abdelrhman, A. M., 2013, "Wavelet Analysis: Mother Wavelet Selection Methods," Appl. Mech. Mater., **393**, pp. 953–958.

[49]   Saito, N., 1994, "Simultaneous Noise Suppression and Signal Compression using a Library of Orthonormal Bases and the Minimum Description Length Criterion," WAVELETS Geophys., pp. 299–324.

[50]   Pereira, M. P., Duncan, J. L., Yan, W., and Rolfe, B. F., 2009, "Contact pressure evolution at the die radius in sheet metal stamping," J. Mater. Process. Technol., **209**(7), pp. 3532–3541.

[51]   Petropoulos, G. P., Pandazaras, C. N., and Davim, J. P., 2010, "Surface Texture Characterization and Evaluation Related to Machining," Surface Integrity in Machining, Springer London, London, pp. 37–66.

[52]   Mendenhall, W., and Sincich, T., 2016, Statistics for engineering and the sciences, CRC Press, Boca Raton, FL.

[53]   Kuzinovski, M., and Tomov, M., 2009, "Effect of sampling spacing upon change of hybrid parameters values of the roughness profile," J. Prod. Eng., **12**(1), pp. 23–28.

[54]   Nie, X., Wang, L., Yao, Z. C., Zhang, L., and Cheng, F., 2005, "Sliding wear behaviour of electrolytic plasma nitrided cast iron and steel," Surf. Coatings Technol., **200**(5), pp. 1745–1750.

Highlights

•   Definition of a new method for galling severity measurement on sheet metal parts.
•   Discrete wavelet transform decomposition is used to measure galling wear severity.
•   Case study showing defined method out performs previous measures of galling wear.
•   Method provides targeted, repeatable and non-subjective galling severity measure.